

Adaptive Microwave Photonic Spectral Shaper for RF Response Tailoring

Qidi Liu and Mable P. Fok*

Lightwave and Microwave Photonics Laboratory, College of Engineering,
The University of Georgia, Athens, Georgia, 30602, USA

*Corresponding author: mfok@uga.edu

Abstract: A photonic-enabled fully-programmable RF spectral shaper capable of point-by-point precise manipulation of wideband RF spectrum with 30-MHz resolution is experimentally demonstrated. Over 10 spectral-control points are achieved with the optimized spectral decomposition and reconstruction algorithm.

OCIS codes: (060.5625) Radio frequency photonics; (350.4010) Microwaves; (070.2615) Frequency filtering.

1. Introduction

Dynamic microwave spectral shaper that is capable of precisely and adaptively processing wideband RF spectrum in a point-by-point manner is essential in realizing high fidelity, reliable, and high-capacity RF systems, including multiband satellite and radar systems, multi-service mobile communication, as well as emerging 5G/6G RF systems. Due to the inherent limitation of RF electronics, undesired RF response is unavoidable as a result of the accumulated uneven gain/loss curve of various RF components and RF channels at different bands. Furthermore, multi-carrier transmissions have their carrier frequency spread across a wide frequency range, making it very challenging to avoid signal degradation and obtain consistent transmission performance among carriers at different frequency [1]. Therefore, there is a critical need for a dynamic RF spectral shaper that is capable of precisely and adaptively shaping and equalizing the wideband RF spectrum to guarantee a high quality and reliable RF transmission performance. Unfortunately, RF electronics is only capable of performing simple spectral filtering tasks using a combination of cascaded attenuators, switches, and filters, due to its tight design criteria, resulting in limited frequency/amplitude control, simple and single-point shaping functions, as well as the inability to adapt to dynamic application scenarios. Turning to photonics for solution, recent development of multiband microwave photonic filters [2,3] paves a promising path towards point-by-point RF spectral shaping. Existing multiband filters mostly have fixed spectral properties, while some of them are capable of center frequency tuning. In order to achieve dynamic, adaptive, and precise manipulation of wideband RF spectrum, user-defined spectral control points, as well as independent and multi-degree of freedom tunability at each spectral control point is necessary.

In this paper, we propose and demonstrate a photonic-enabled dynamic RF spectral shaper that can be fully programmable to perform precise point-by-point wideband spectral shaping with a 30-MHz resolution. The RF spectral shaper is capable of dynamic frequency response tuning through the use of an adaptive and optimized RF response decomposition/reconstruction algorithm as well as a microwave photonic based reconfigurable multi-point RF spectral control hardware [4,5]. The demonstrated RF spectral shaper is capable of adapting to any target RF response as well as providing dynamic configuration range based on the desired spectral response.

2. Principle and Experimental Setup

Figure 1 shows the experimental setup of the proposed RF spectral shaper. A superluminescent diode (Thorlabs SLD S5FC1005S) is utilized as a broadband optical carrier, which covers the wavelength range from 1528 nm to 1568 nm. An optical wave shaper (Finisar 1000S) is used for controlling the optical carrier property through optical spectral slicing, carrier amplitude controlling, and bandwidth limiting, based on the RF spectral decomposition and reconstruction algorithm. A 12-GHz electro-optic modulator (Fujitsu FTM7921ER) is used to modulate the wideband RF information onto the sliced optical carriers. In this experiment, output of the network analyzer is used as the RF

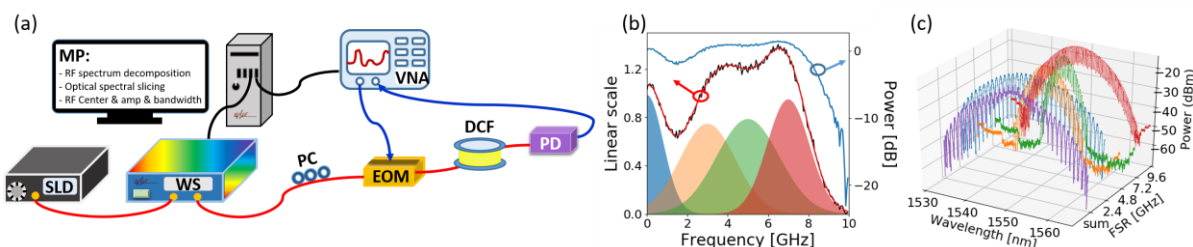


Fig. 1. (a) Experimental setup of the point-by-point RF spectral shaper. SLD: superluminescent diode; WS: optical wave shaper; PC: polarization controller; EOM: electro-optic modulator; DCF: dispersion compensating fiber; VNA: vector network analyzer. MP: microprocessor (Red line: optical paths; blue line: electrical paths; black line: USB cables); (b) Illustration of the RF spectral decomposition and reconstruction process (red curve: target RF response, black curve: reconstructed RF response, blue curve: reconstructed RF response in log scale.); (c) Decomposition and summation of optical spectra for various spectral control points.

signal for characterization of the RF spectral shaper. Next, a piece of dispersion compensating fiber with total dispersion of 397.35 ps/nm is used to introduce proper wavelength dependent delay to the spectrally sliced optical carriers. An 18-GHz photodetector is used to convert the optical signal to the RF domain and the resultant RF response is measured by a 20-GHz vector network analyzer (Agilent E5071C). The heart of the proposed fully programmable RF spectral shaper is a two-section algorithm for optimized RF spectral decomposition and RF spectral reconstruction.

RF Spectral Decomposition and Optimization

Similar to a time domain waveform that any repetitive signal can be decomposed into a series of sinusoids at different frequencies, RF spectrum can be described by a composition of Gaussian functions with different bandwidth and amplitude, with the Gaussian peaks align at the maxima of the RF spectrum and tails of Gaussian functions could overlap and reconstruct the minima. Therefore, a widely spaced subset of Gaussian functions with wide bandwidth will lead to a gentle change in the resultant RF spectral response with coarse spectral control, while a closely spaced subset of Gaussian functions with narrow bandwidth will lead to a steep change in the resultant RF spectral response with fine spectral control. Furthermore, overlapping regions between each Gaussian functions could constitute the amplitude of a RF spectral valley or plateau. Thus, given a target RF spectral function (e.g. complementary RF response for equalization), a sum of Gaussian functions can be used to represent the target RF spectral function, as shown in Fig. 1(b). The number of Gaussian functions corresponds to the number of control points in the RF spectrum. Algorithm 1 depicts the identification and optimization of the resultant Gaussian functions. Mathematical expression of the group of Gaussian functions is,

$$F_R(f) = \sum_{i=1}^n C_i \exp\left[-\frac{(f - f_{c-i})^2}{2f_{3dB-i}^2}\right] \quad (1)$$

where n is the total number of Gaussian functions for RF spectral reconstruction, C_i , f_{c-i} and f_{3dB-i} are the amplitude, center frequency, and 3-dB bandwidth of the i^{th} Gaussian function. The discrepancy between the target RF response and the reconstructed RF response could be reduced using a large number of Gaussian functions, however an overly large number of Gaussian functions could consequently degrade the optical spectra for RF response reconstruction. Therefore, first part of the algorithm also identifies the optimized number of Gaussian functions needed while keeping the discrepancy within the set error limit. Therefore, the value of n is determined by the optimal number of Gaussian functions for RF response reconstruction to achieve discrepancy within the error tolerance ε , that is governed by

$$\sqrt{\frac{1}{N} \sum_{k=1}^N (F_R(f_k) - p_k)^2} < \varepsilon \quad (2)$$

where N is the total number of frequency sampling points for describing the target RF function, p_k is the power magnitude of the k^{th} frequency sampling point, and $F_R(f_k)$ is the fitted power function of the k^{th} power that contributes to maintaining the RF response discrepancy within ε .

RF Spectral Reconstruction Once the RF spectral decomposition algorithm has determined all the parameters for the set of Gaussian functions, second part of the algorithm for RF spectral reconstruction will determine the corresponding optical parameters, including the number of interleaving optical combs, the bandwidth of each optical comb, the general envelope profile and amplitude (red, green, blue, and orange curves in Fig. 1(c)), as well as the final optical spectral function (purple curve in Fig. 1(c)). Since the Gaussian functions in the RF domain $F_R(f)$ and the corresponding optical profile $H_n(\omega)$ for that particular spectral control point has a Fourier transform relationship, therefore, the aggregated final optical spectral function $T(\omega)$ can be expressed as a summation of cosine functions with Gaussian envelope $H_n(\omega)$ as shown in Eq. (3):

$$T(\omega) = \sum_{n=1}^N A_n \cos\left(\frac{\Delta\omega_n}{\Delta\omega_{FSR-n}} \frac{\omega}{2}\right) H_n(\omega) \quad (3)$$

where A_n is the amplitude of the n^{th} optical comb (corresponding to the n^{th} Gaussian function/RF control point), $\Delta\omega_n$ is the full bandwidth of the shaped optical spectrum, and $\Delta\omega_{FSR-n}$ is the designed free spectrum range (FSR) of each sliced optical carriers. It is worth to notice that our scheme is different from the optical spectral shaping to RF spectral mapping approach that has coarse spectral resolution of 12 GHz. The unique advantage of our proposed RF spectral

Algorithm 1. RF Spectral Decomposition and Optimization

1. *input*: data of RF response curve $\{(f_k, p_k): k = 1, \dots, N\}$
2. determine and label m maxima and minima of the data
3. estimate the parameters of the m Gaussian basis
4. set $n = 1$
5. **if** $n > m$ then stop
 - else** use the parameters of n most dominant Gaussians determined in step 3 as the initial values for the Marquardt algorithm and refine the parameters.
6. **If** the resultant error $e_n < \varepsilon$ then stop
 - else** increasing n by one and go to step 5.
7. *output*: the number of n and the corresponding parameters $\{C_i, f_{c-i}, f_{3dB-i}: i = 1, \dots, n\}$ of each Gaussian functions

shaper is the ability of being fully programmable and the point-by-point control capability with 30 MHz step resolution based on dispersion-induced microwave photonic finite impulse response.

3. Results and Discussion

Fig. 2 shows the experimental results of the programmable point-by-point RF spectral shaper. First, the target RF response is defined by the user – indicated by the red curve in Fig. 2(a). Our proposed algorithm decomposes the target RF response into a number of Gaussian functions, as shown by the five colored Gaussian shapes at 2.4 GHz, 3.8 GHz, 5.8 GHz, 7.8 GHz and 8.5 GHz in Fig. 2(a). The number of Gaussian functions is optimized to use the minimal Gaussian functions for obtaining RF response matching within the set error limit. The parameters of the Gaussian functions are fed to the 2nd part of the algorithm to generate the corresponding optical parameter for controlling the hardware of the RF spectral shaper. After photodetection, the reconstructed RF response in linear scale is shown by the black curve in Fig. 2(a). The target response here is designed by the user for supporting Bluetooth/WiFi transmission as well as gain equalization at high frequency regions. Fig. 2(b) shows a comparison between the target RF response and the shaped RF response in log scale. The discrepancy is small - indicated by the green shaded region. Region I is a Bluetooth/ WiFi transmission window at 2.4 GHz with 40-dB rejection ratio, while Region II and III are the spectral compensation region with 10 dB and 6 dB dynamic shaping range, respectively. Furthermore, we use the above algorithm to generate various target RF responses with different properties. Showing in Fig. 2(c) are several examples including negative linear response with variable slopes (magenta and black), positive slopes (sky blue), sinusoid (orange), and bandpass-shaping (brown and purple).

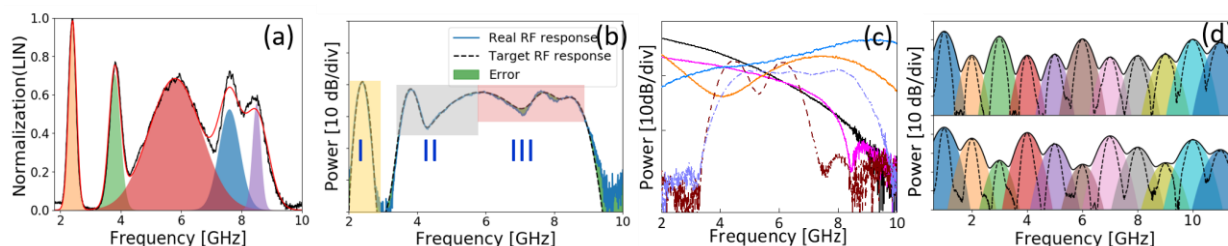


Fig. 2. (a) Experimental results of the RF spectrum optimized decomposition and reconstruction algorithm - target RF response (red curve), reconstructed RF response (black curve), set of Gaussian functions (shaded); (b) Target RF response for simultaneous bluetooth/wifi channel filtering (region I) and spectral compensation (region II and III), mismatch are showed in red shade; (c) Samples of various target RF responses achieved by the RF spectral shaper; (d) Eleven spectral control points reconstructing a target RF response.

To prove the ability to perform high spectral control point count for point-by-point spectral shaping, bandwidth of each Gaussian function is intentionally set to be narrow (3-dB bandwidth of 220 MHz) and Gaussian functions are evenly spaced at 1 GHz so that we can clearly see each of the peaks, i.e. no overlapping between peaks. Peaks of the Gaussian functions can be placed as close as 30 MHz if needed, governed by the resolution of optical spectral slicing and the dispersion of dispersion compensation fiber. Fig. 2(d) shows two examples of the target RF response in solid black curves, with dashed line showing the position of the decomposed Gaussian functions, and the shaded regions showing the reconstruction of the RF response when wide Gaussian functions are used.

4. Conclusion

A point-by-point adaptive and programmable RF spectral shaper has been proposed and experimentally demonstrated, controlled by a two-section algorithm for optimized RF spectral decomposition and reconstruction. The resultant frequency response of the RF spectral shaper is highly tunable and adaptive to the changing RF environment. Over 10 individually customizable RF spectral control points with 30 MHz resolution have been obtained to reconstruct the target RF response.

Acknowledgment

This work is supported by National Science Foundation (1653525 and 1917043).

References

- [1] Hueber, Gernot, and Robert Bogdan Staszewski. Multi-Mode/Multi-Band RF Transceivers for Wireless Communications. Hoboken, New Jersey: John Wiley & Sons, 2011.
- [2] M. P. Fok, J. Ge, and Q. Liu, "Dynamic and multiband RF spectral processing," in *Smart Photonic and Optoelectronic Integrated Circuits XXI*, vol. 10922 (International Society for Optics and Photonics, 2019), pp. 109221D.
- [3] K. Hyoungh-Jun, D. E. Leaird, and A. M. Weiner, "Rapidly tunable dual-comb RF photonic filter for ultrabroadband RF spread spectrum applications." *IEEE Trans. Microw. Theory Tech.* **64**, 3351-3362(2016).
- [4] J. Ge, D. A. Garon, and M. P. Fok, "Photonic implementation of a highly reconfigurable wideband RF spectral shaper." *Opt. Commun.* **445**, 111-118 (2019).
- [5] Q. Liu, J. Ge, and M. P. Fok, "Microwave photonic multiband filter with independently tunable passband spectral properties." *Opt. Lett.* **43**, 5685-5688 (2018).